Supporting Information

Synthesis, Biophysical Studies and RNA Interference Activity of RNA Having Three Consecutive Amide Linkages

Paul Tanui,[†] Scott D. Kennedy,[‡] Benjamin D. Lunstad,[§] Amanda Haas,[§] Devin Leake[§] and Eriks Rozners*[,†]

[†]Department of Chemistry, Binghamton University, The State University of New York, Binghamton, New York 13902

[‡]Department of Biochemistry and Biophysics, University of Rochester School of Medicine and Dentistry, Rochester, New York 14642

[§]Global Research and Development in Molecular Biology, Thermo Fisher Scientific Bioscience Division, Lafayette, Colorado 80026

Table of contents

Experimental Procedures

Methylene chloride, pyridine, acetonitrile, and toluene were dried by refluxing with CaH_2 followed by distillation. Tetrahydrofuran was distilled from sodium/benzophenone ketyl. Reactions were carried out in oven (150 ^oC) dried glassware under an atmosphere of dry nitrogen. NMR spectra were recorded on a Bruker AM360 spectrometer at ambient temperature. Thin layer chromatography (TLC) was performed on Silacycle 0.25 mm 60 Å silica gel F_{254} plates. Column chromatography was done on SiliaFlash® P60 230-400 mesh silica gel (Silacycle).

5′-Azido-5′-deoxy-2′-*O*-triisopropylsilyloxymethyluridine. Diisopropylethylamine (2.86 mL, 16.4 mmol) was added to a solution of 5′-azido-5′-deoxyuridine **2**[1] (1.36 g, 4.2 mmol) in dichloroethane (50 mL). Bu_2SnCl_2 (1.69 g, 5.47 mmol) was added and the reaction mixture was stirred for 1 h at room temperature. Triisopropylsiloxymethyl chloride (1.38 g, 5.97 mmol) was added and the resulting solution was stirred at 80 °C for 0.5 h, cooled to room temperature, and concentrated under reduced pressure. The residue was dissolved with dichloromethane (100 mL) and washed with water (100 mL). The organic layer was dried over Na_2SO_4 and concentrated under reduced pressure. The crude residue was purified via silica gel column chromatography eluting with a stepwise gradient of 10-50% ethyl acetate in hexane (containing 1% triethylamine) to afford 0.63 g (36%) of the desired 2′-*O*-(triisopropylsilyloxy)methyl isomer as a white foam. ^1H NMR ($CDCl_3$) δ: 7.55 (d, J = 8.1 Hz, 1H), 5.89 (d, J = 3.9 Hz, 1H), 5.77 (d, J = 8.1 Hz, 1H), 5.14 (d, J = 5.1 Hz, 2H), 4.95 (d, J = 4.7 Hz, 2H), 4.24 (m, 1H), 4.13 (m, 1H), 4.07 (m, 1H), 3.78 (dd, J = 13.2 and 2.6 Hz, 1H), 3.64 (dd, J = 13.2 and 3.4 Hz, 1H), 1.04 (m, 21H). ^{13}C NMR ($CDCl_3$) δ: 163.3, 150.2, 140.0, 102.8, 90.6, 89.2, 82.1, 81.6, 69.7, 51.7, 17.6, 11.7.

5′-Amino-5′-deoxy-2′-*O*-triisopropylsilyloxymethyluridine (5). H_2S gas was passed through a stirred solution of 5′-azido-5′-deoxy-2′-*O*-triisopropylsilyloxymethyluridine (0.61 g, 1.34 mmol) in pyridine (60 mL) and water (15 mL) for one hour. The reaction mixture was stirred overnight at room temperature, volatiles were removed under vacuum and the residue was purified by silica gel column chromatography eluting with a stepwise gradient of 3-10% methanol in CH_2Cl_2 containing 1% aqueous ammonia) to give 506 mg (88%) of **5**. ^1H NMR ($CDCl_3$) δ: 7.39 (d, J = 7.7 Hz, 1H), 5.64 (d, J = 3.8 Hz, 1H), 5.60 (d, J = 8.1 Hz, 1H), 4.98 (d, J = 5.1 Hz, 1H), 4.89 (d, J = 4.7 Hz, 1H), 4.26 (m, 1H), 3.96 (m, 1H), 2.92 (m, 1H), 2.80 (m, 1H), 0.95 (m, 21H). ^{13}C NMR ($CDCl_3$) δ: 164.0, 150.2, 141.4, 102.3, 90.5, 90.1, 84.4, 80.1, 70.0, 42.7, 17.4, 11.6.

[1] Yamamoto, I.; Sekine, M.; Hata, T. *J. Chem. Soc., Perkin Trans. 1*. **1980**, 306-310.

5′-Deoxy-5′-methoxytritylamino-2′-triisopropylsilyloxymethyluridine. 5′-Amino-5′-deoxy-2′-*O*-triisopropylsilyloxymethyluridine **5** (200 mg, 0.466 mmol) was dissolved in anhydrous pyridine (8 mL) at 0 ^{0}C and methoxytrityl chloride (717 mg, 2.33 mmol) was added. The solution was stirred at room temperature overnight. The reaction was quenched with saturated aqueous triethylammonium bicarbonate (0.8 mL) and evaporated in vacuum. The residue was dissolved in CH_2Cl_2 (40 mL) and extracted with saturated aqueous $NaHCO_3$ (3 × 40 ml). The organic phase was dried with Na_2SO_4, filtered and concentrated in vacuum. The residue was purified using silica gel column chromatography eluting with a stepwise gradient of 0-10% methanol in CH_2Cl_2 containing 100 ppm of triethylamine to give 251 mg, 0.359 mmol (77 %) of the title compound. ^{1}H NMR ($CDCl_3$, 300 MHz) δ 7.53-7.14 (m, 14H), 6.82 (d, *J* = 8.3 Hz, 2H), 5.76 (d, *J* = 3.9 Hz, 1H), 5.64 (d, *J* = 8.1 Hz, 1H), 5.08 (d, *J* = 4.7 Hz, 1H), 4.96 (d, J = 4.7 Hz, 1H), 4.32-4.24 (m, 2H), 4.16 (t, *J* = 7.0 Hz, 1H), 3.77 (s, 3H), 2.74-2.64 (m, 1H), 2.42-2.37 (m, 1H), 1.08 (m, 23H).

Phosphoramidite 1. 5′-Deoxy-5′-methoxytritylamino-2′-triisopropylsilyloxymethyluridine (250 mg, 0.356 mmol) was co-evaporated with dry acetonitrile (3 × 5 mL) and dissolved in dry CH_2Cl_2 (2 mL). Diisopropylethylamine (248 μL, 1.42 mmol) was added followed by careful and slow addition of 2-cyanoethyl *N,N*-diisopropylchlorophosphoramidite (87 μL, 0.392 mmol) and stirred the reaction mixture for 14 hours under slow stream of nitrogen. The reaction was concentrated under reduced pressure and the crude product was purified using silica gel column chromatography eluting with a stepwise gradient of MeOH (0-3%) in CH_2Cl_2 containing 100 ppm of triethylamine to give 196 mg, 0.217 mmol (61 %) of phosphoramidite **1**. ^{1}H NMR (CD_3CN, 600 MHz) δ 9.22 (bs, 1H), 7.52 – 7.20 (m, 15H), 6.88 (m, 2H), 5.88 (d, *J* = 4.76 Hz, 1H), 5.62 (d, *J* = 6.12 Hz, 1H), 5.04 (q, *J* = 7.9 Hz, 1H), 4.29 (t, *J* = 5.1 Hz, 1H), 4.17 (t, *J* = 5.0 Hz, 1H), 4.11 – 4.00 (m, 2H), 3.79 (s, 3H), 3.54 – 3.29 (m, 1H), 2.53 – 2.46 (m, 1H), 2.37 – 2.11 (m, 4H), 2.00 (m, 1H), 1.08 (m, 28H); ^{13}C NMR (CD_3CN, 150 MHz) δ 162.5, 157.8, 150.0, 145.9, 140.4, 137.6, 129.6, 129.5, 128.8, 127.5, 126.0, 112.7, 102.1, 89.2, 87.7, 83.6, 78.7, 70.0, 69.8, 59.7, 54.6, 45.2, 16.9, 11.4. ^{31}P NMR (CD_3CN) δ: 149.7 and 149.5.

2′-*O-tert*-Butyldimethylsilyl-3′,5′-dideoxy-3′-carboxymethyl-5′-methoxytritylaminouridine triethylammonium salt (2b). Hydrogen sulfide gas was passed through a solution of 5′-azido-2′-*O-tert*-butyldimethylsilyl-3′,5′-dideoxy-3′-carboxymethyl-5′-methoxytritylaminouridine **7b** (302 mg, 0.78

mmol, prepared following our published procedures[2]) in pyridine/water (30 mL, 4:1 v/v) at room temperature for 1 h. The solution was stirred overnight and evaporated in vacuum. The residue was dissolved in water (55 mL) and washed with CH_2Cl_2 (4 × 55 mL). The organic layers were discarded and the water phase was evaporated to give the amine intermediate (~297 mg, ~0.74 mmol, ~94%), which was used in the next step without further purification. The amine intermediate was dissolved in anhydrous pyridine (13 mL) and methoxytrityl chloride (1.12 g, 3.62 mmol) was added. The solution was stirred at room temperature overnight. The reaction was quenched with saturated aqueous triethylammonium bicarbonate (1.3 mL) and evaporated in vacuum. The residue was dissolved in CH_2Cl_2 (65 mL) and extracted with saturated aqueous $NaHCO_3$ (3 × 65 mL). The organic phase was dried with Na_2SO_4, filtered and concentrated in vacuum. The residue was purified using silica gel column chromatography eluting with a stepwise gradient of methanol (0-10%) in CH_2Cl_2 containing 100 ppm of triethylamine to give the title compound **2b** (422 mg, 0.54 mmol, 70% for two steps). ^{1}H NMR (CD_3CN, 600 MHz) δ 10.37-8.98 (s, 2H), 8.08 (d, *J*= 7.95 1H), 7.38 (d, 4H), 7.27 (d, 2H), 7.18 (t, 4H), 7.09 (t, 2H), 6.74 (d, *J*= 7.55 Hz, 2H), 5.47 (s, 1H), 5.22 (d, *J*= 7.99, 1H), 4.30 (s, 1H), 3.93 (m, 1H), 3.63 (s, 3H), 2.62 (q+m, 12H), 2.36 (m, 1H), 2.24 (m, 1H), 2.13 (m, 1H), 0.90 (t, 15H), 0.79 (s, 9H), 0.10 (s, 3H), 0.00 (s, 3H). ^{13}C NMR (CD_3CN, 150 MHz) δ 177.9, 165.1, 159.4, 151.9, 147.9, 147.8, 141.5, 139.5, 130.0, 129.1, 127.6, 114.4, 102.0, 93.2, 85.9, 80.4, 71.7, 56.2, 46.5, 46.4, 41.2, 33.3, 26.8, 19.1, 10.6, 10.5, -3.5, -4.6.

Synthesis of amide-modified RNA1-RNA4 started as standard 1 μmol scale RNA phosphoramidite synthesis protocol on an Expedite Model 8909 Nucleic Acid Synthesis System. First the 3′-end phosphodiester linkages were assembled using commercially available (Glen Research) C or U synthesis columns and 2′-*O*-TOM protected phosphoramidites then monomer **1** was used to introduce the 5′-amino group. The synthesis column was removed from Expedite and equipped with a 1 mL plastic syringe at each end as described in Expedite manual for post-synthetic operations. In a separate vial monomers **2b** or **3b** (10.9 mg, 15.6 μmol), HATU (3.95 mg, 10.4 μmol), and diisopropylethylamine (2.7 μL) were mixed in dry DMF (80 μL) under nitrogen for 5 minutes. The solution was added to the column via one of the syringes. The solution was pushed back and forth a couple of times though the column using the two attached syringes and left on an orbital shaker for 8 h. The solution was pushed out of the column and the column was washed successively with dry DMF (2 × 1 mL), methanol (2 × 1 mL) and CH_2Cl_2 (2 × 1 mL). The unreacted amino groups were capped by treating the column with a mixture

[2] Tanui, P.; Kullberg, M.; Song, N.; Chivate, Y.; Rozners, E. *Tetrahedron* **2010**, *66*, 4961-4964; Rozners, E.; Liu, Y. *Org.*

of acetic anhydride, 2,6-lutidine and DMF (5:16:79, v/v, 0.5 mL) for 10 min. The capping solution was removed and the column was washed successively with dry DMF (3 × 1 mL), methanol (3 × 1 mL) and CH_2Cl_2 (3 × 1 mL). The methoxytrityl group was removed by treating the support with trifluoroacetic acid in CH_2Cl_2 (3 % v/v, 1 mL) for 10 minutes. The column was washed with trifluoroacetic acid in CH_2Cl_2 (3 % v/v, 1 mL) and CH_2Cl_2 (1 mL). The yellow-orange wash solutions were combined and used to estimate the coupling yields based on spectrophotometric comparison of the intensity of methoxytrityl cation at 478 nm. The column was washed successively with DMF (2 × 1 mL), methanol (2 × 1 mL) and CH_2Cl_2 (2 × 1 mL), dried under a stream of nitrogen and was ready for the next coupling step. The synthetic cycle was repeated until the required number of amide linkages was introduced and the column was transferred back to the Expedite synthesizer to complete the phosphodiester portion of amide-modified RNAs. After completion of the synthesis, the support was split in half. One half was deprotected as described below. The other half was 5'-phosphorylated using Chemical Phosphorylation Reagent II (Glen Research) and following manufacturers recommendations, before depreotection.

Cleavage of amide-modified RNA from solid support and deprotection. The synthesis column was treated with 7 N methanolic ammonia (1 mL) for 2 h followed by decanting and washing the support with methanolic ammonia solution (0.5 mL). The ammonia solutions were combined and left at room temperature for 2 days to complete the deprotection of nucleobases. The solution was evaporated, the residue was dissolved in DMSO (100 μL) and triethylamine trihydrofluoride (125 μL) was added. The solution was left for 24 h at room temperature. The reaction mixture was diluted with water (1.275 mL) and desalted on Sephadex C25 according to the manufacturer's recommendation. The oligonucleotides were purified by RP-HPLC using Supelco-C18 column (4.6 × 150 mm, 5 μm) with linear gradient of acetonitrile (2-10%) in 0.1 M triethylammonium acetate buffer (pH 7.0, 65 ^{o}C), flow rate 1 mL/min. The residue was lyophilized several times to remove triethylammonium acetate. The structures of **RNA1-RNA4** were confirmed by ESI mass spectrometry and that of **RNA1** also by the NMR spectroscopy, see below. Oligonucleotide concentrations were calculated using extinction coefficients obtained using the nearest-neighbor approximation.[3] Unmodified RNA complementary to **RNA1** was purchased from Thermo Fisher Scientific and purified by HPLC as described above.

Lett. **2003**, *5*, 181-184; Rozners, E.; Liu, Y. *J.Org.Chem.* **2005**, *70*, 9841-9848.
[3] Puglisi, J.D.; Tinoco, I., Jr. *Methods in Enzymology* **1989**, *180*, 304-324.

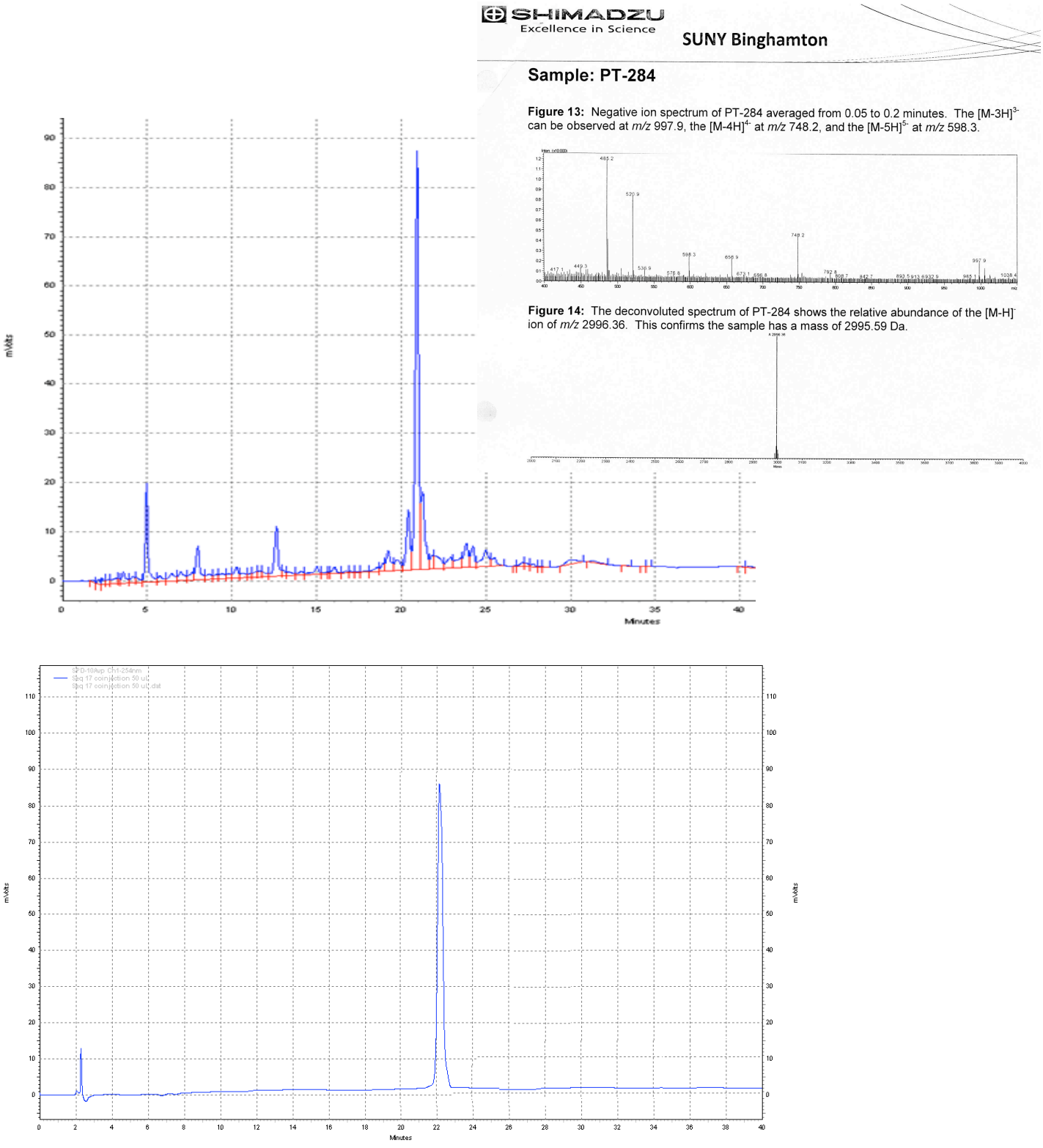

Figure S1. HPLC chromatograms of **RNA1** ($^{5'}$-GpCpGpUaUaUaUpCpGpC-$^{3'}$): crude synthesis mixture (upper panel) and analysis of purified **RNA1** (lower panel). The ESI LC-MS (upper right) analysis confirms that the product has the expected mass of 2995.59 Da. To produce enough material for NMR studies, synthesis of **RNA1** was repeated four times with overall yields of 24 (2%), 54 (5%), 29 (3%), and 9 (1%) nmols.

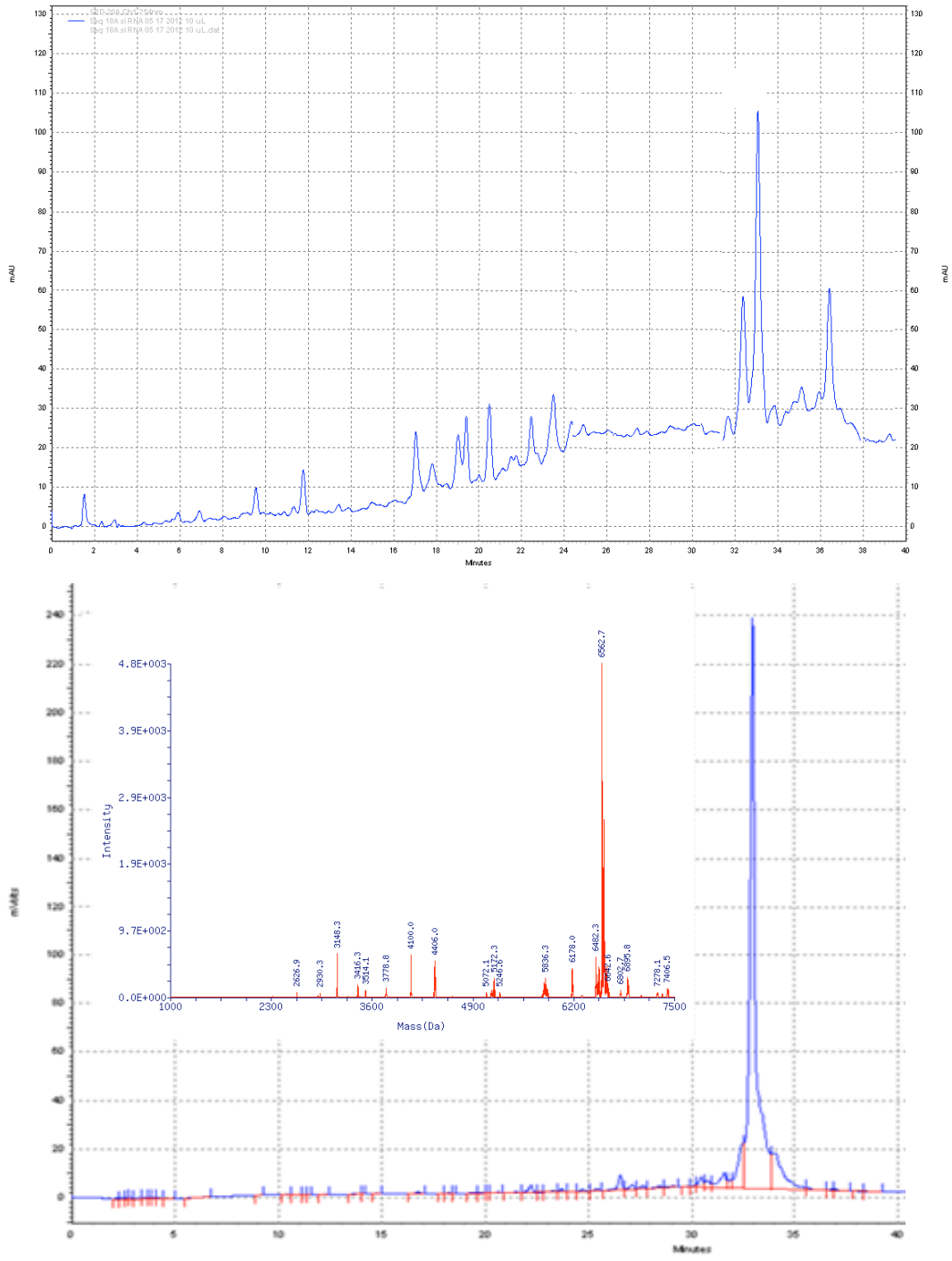

Figure S2. HPLC chromatograms of **RNA2**, 5′-phosphorylated ($^{5'}$-pUpApUaUaUaUpGpApCpCpUpApCpGpApApUpUpGpUpU$^{-3'}$): crude synthesis mixture (upper panel) and analysis of purified **RNA2** (lower panel). Yield 1.1 nmols, 0.2%. Inset: ESI MS confirms that the product has a mass of 6562.7 Da; calculated mass 6562.1 Da. Major impurity at 36.2 min, mass 5086.3 Da corresponds to $^{5'}$-AcNH-UpGpApCpCpUpApCpGpApApUpUpGpUpU$^{-3'}$; calculated mass 5086.1.

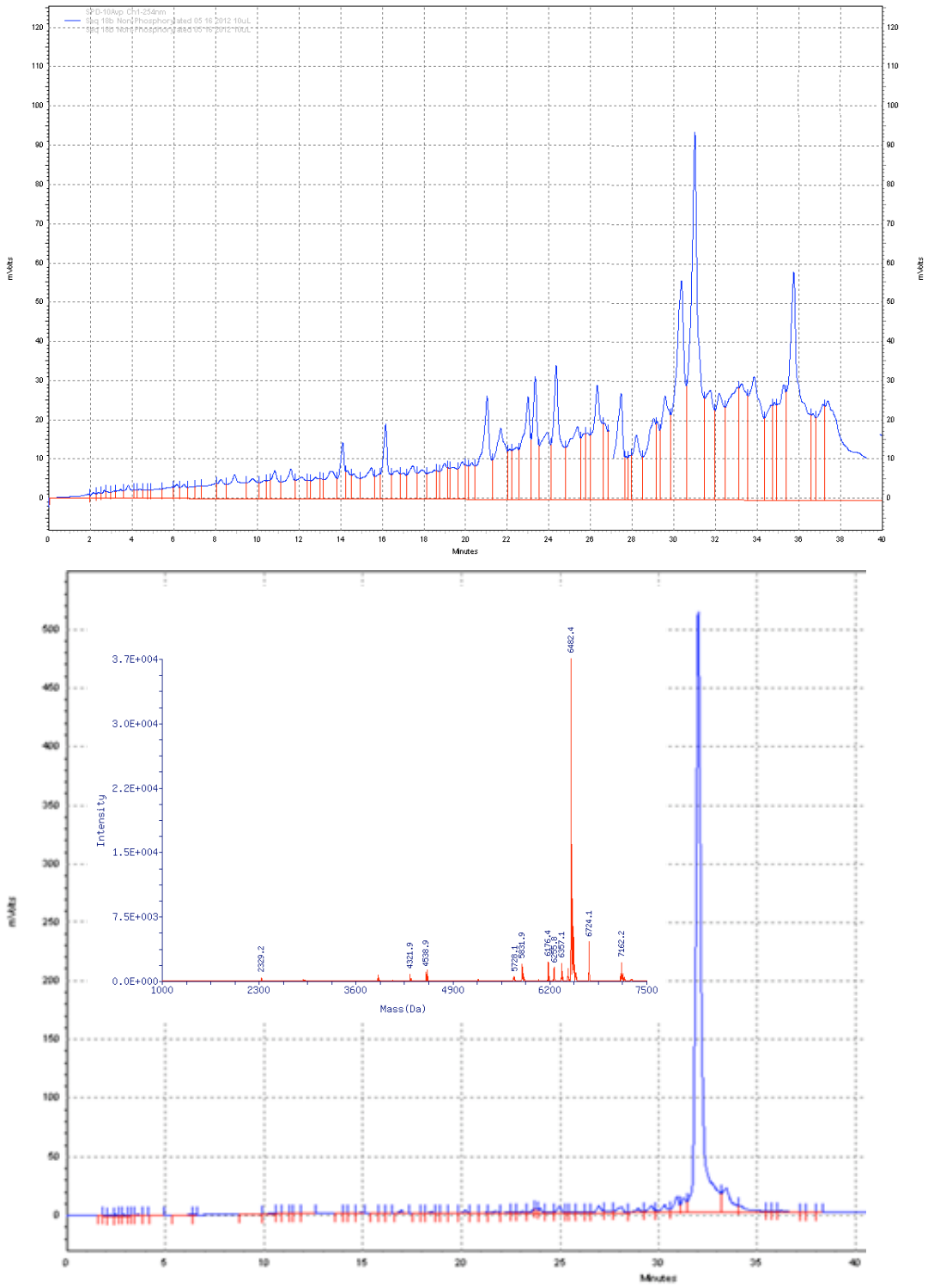

Figure S3. HPLC chromatograms of **RNA2**, 5′-OH ($^{5'}$-UpApUaUaUaUpGpApCpCpUpApCpGpApApUpUpGpUpU-$^{3'}$): crude synthesis mixture (upper panel) and analysis of purified **RNA2** (lower panel). Yield 6 nmols, 1.2%. Inset: ESI MS confirms that the product has a mass of 6482.4 Da; calculated mass 6482.1 Da. Major impurity at 35.8 min, mass 5086.7 Da corresponds to $^{5'}$-AcNH-UpGpApCpCpUpApCpGpApApUpUpGpUpU-$^{3'}$; calculated mass 5086.1.

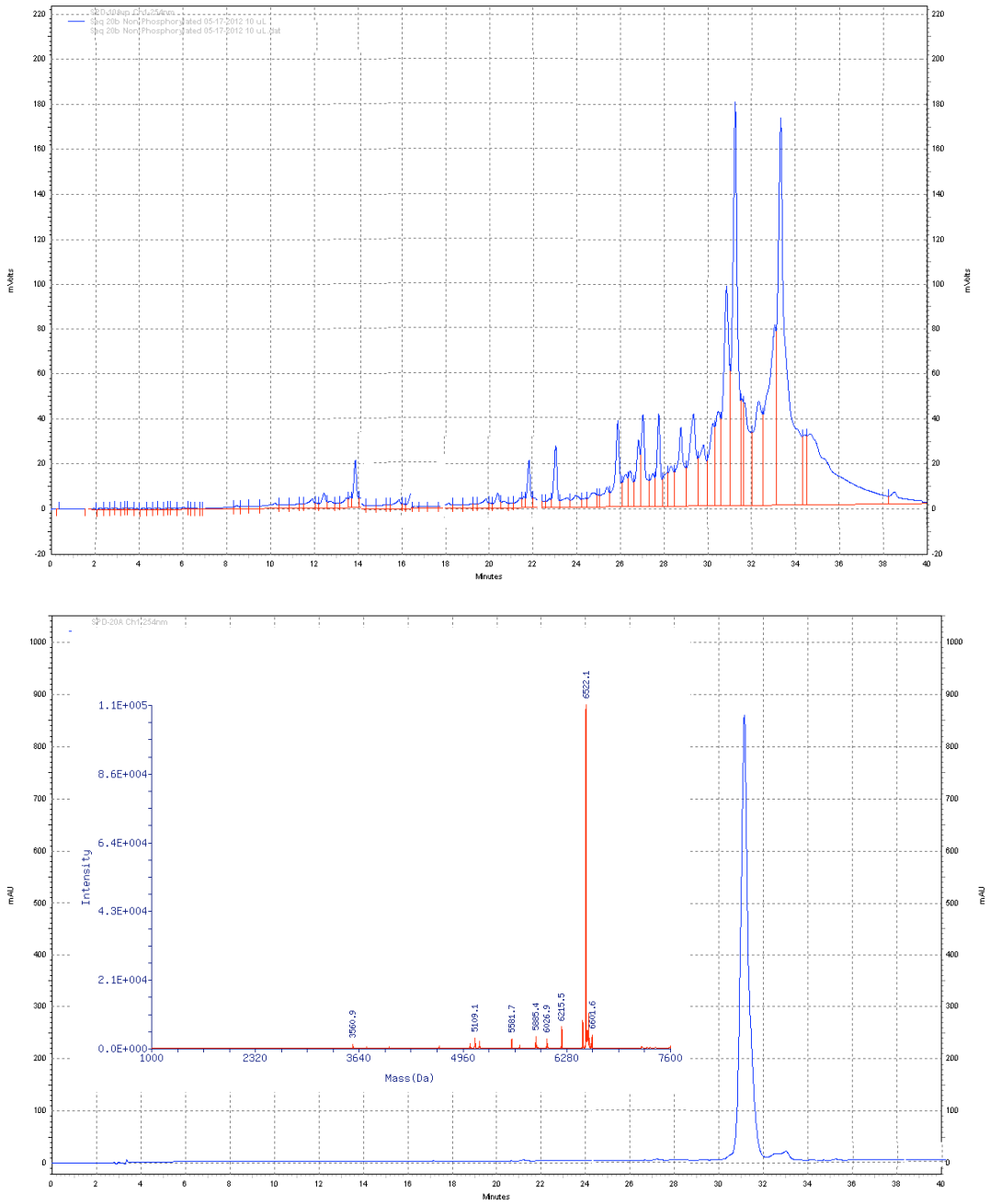

Figure S4. HPLC chromatograms of **RNA3**, 5′-OH ($^{5'}$-UpApUpUaUaUpGpApCpCpUpApCpGpApApUpUpGpUpU$^{-3'}$): crude synthesis mixture (upper panel) and analysis of purified **RNA3** (lower panel). Yield 5 nmols, 1%. Inset: ESI MS confirms that the product has a mass of 6522.1 Da; calculated mass 6521.0 Da. Major impurity at 33.4 min, mass 5085.8 Da corresponds to $^{5'}$-AcNH-UpGpApCpCpUpApCpGpApApUpUpGpUpU $^{-3'}$; calculated mass 5086.1.

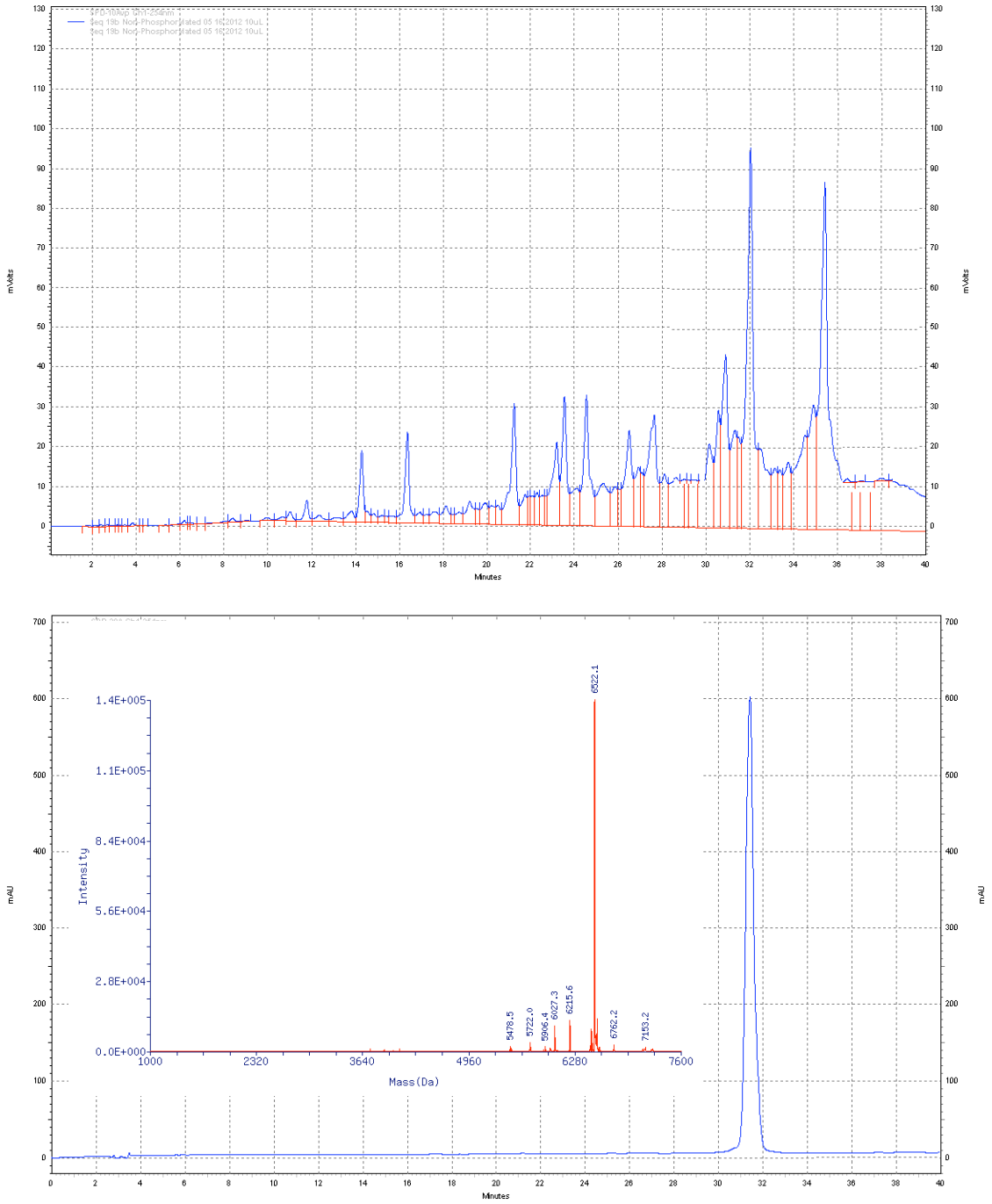

Figure S5. HPLC chromatograms of **RNA4**, 5′-OH ($^{5'}$-UpApUaUaUpUpGpApCpCpUpApCpGpApApUpUpGpUpU$^{-3'}$): crude synthesis mixture (upper panel) and analysis of purified **RNA4** (lower panel). Yield 3 nmols, 0.6%. Inset: ESI MS confirms that the product has a mass of 6522.1 Da; calculated mass 6521.0 Da. Major impurity at 35.5 min, mass 5392.4 Da corresponds to $^{5'}$-AcNH-UpUpGpApCpCpUpApCpGpApApUpUpGpUpU$^{-3'}$; calculated mass 5392.3.

Table S1. UV thermal melting and osmotic stress data for amide-modified duplex **RNA1**.

File Name	0%Acetamide	5% Acetamide	10% Acetamide	15% Acetamide	20% Acetamide
pt_280A1	48.7		43.4	41.2	39.5
pt_280A2	48.5		42.9	41.5	39.2
pt_280B1	48.9		43.5	41.4	38.5
pt_280B2	49		43.6	41.2	39.2
pt_042A1	48.5	47.2	44.1	41.7	39.8
pt_042A2	48.8	47.5	43.7	41.3	39.9
pt_042B1	48.7	47.3	43.8	41.6	39.9
pt_042B2	48.4	47.4	43.9	41.7	39.7
pt_044A1	48.1	47.2	43.9	41.6	39.9
pt_044A2	48.7	47.3	43.7	41.6	40.1
pt_044B1	48.6	47.4	43.9	41.7	39.8
pt_044B2		46.9	43.8	41.5	39.7
Average	**48.6**	**47.3**	**43.7**	**41.5**	**39.6**
STDEV	**0.2**	**0.2**	**0.3**	**0.2**	**0.4**

File Name	0% Ethylene Glycol	5% Ethylene Glycol	10% Ethylene Glycol	15% Ethylene Glycol	20% Ethylene Glycol
pt_050A1			44.9	43.0	41.3
pt_050A2		45.5	44.6	43.1	41.2
pt_050B1		45.6	45.0	42.6	40.8
pt_050B2		45.1	44.8	42.9	41.0
pt_050C1		45.5		43.1	
pt_050C2		45.3		42.5	
Average		**45.4**	**44.8**	**42.9**	**41.1**
STDEV		**0.2**	**0.2**	**0.3**	**0.2**

File Name	0% Glycerol	5% Glycerol	10% Glycerol	15% Glycerol	20% Glycerol
pt_052A1		46.6	44.9	41.5	41.2
pt_052A2		47.0	44.6	41.6	41.3
pt_052B1		46.5	44.5	41.7	41.4
pt_052B2		46.3	44.2	41.9	40.9
		46.4			
Average		**46.6**	**44.6**	**41.7**	**41.2**
STDEV		**0.3**	**0.3**	**0.2**	**0.2**

	van't Hoff plot		Derivative of α curve			
File Name	ΔH	ΔS	T1	T2	ΔH (cal/mol)	ΔG
pt_280A1	76620	-208.9	41.5	56.5	70231	11.9
pt_280A2	74480	-203.3	42.2	55.6	78602	11.5
pt_280B1	76240	-208	42.3	55.4	79972	11.8

pt_280B2	78900	-217.1	40.1	54.9	70340	11.6
pt_042A1	74880	-204.9	40	54.4	72160	11.4
pt_042A2	73000	-199	40.6	54.7	73905	11.3
pt_042B1	78600	-218	42	56.1	74552	11.0
pt_042B2	78100	-213.5	42.2	56.4	74141	11.9
pt_044A1	74120	-203.5	40.2	54.4	73223	11.0
pt_044A2	77100	-210.5	41.7	55.9	73911	11.8
pt_044B1	75100	-206.5	40.7	54.9	73452	11.1
Average	**76104**	**-208.5**	**41.2**	**55.4**	**74045**	**11.5**
STDEV	**1950**	**5.9**	**0.9**	**0.8**	**2984**	**0.3**

File Name	**2 microM**	**4 microM**	**8 microM**	**16 microM**	**32 microM**
pt_302A	47.2	48.5	50.8	52.2	53.6
	46.9				53.3
pt_302B	47.1	49.1	51.1	52.0	53.4
	46.8				54.0
pt_302C		48.6	50.3	52.4	53.7
	46.7				53.7
pt_303A	47.5	48.1	50.6	52.0	
	47.0		50.7		
pt_303B	47.5	48.0	50.3	52.4	
	46.7		50.2	52.5	
Average	**47.1**	**48.5**	**50.6**	**52.2**	**53.6**
STND DEV	**0.3**	**0.4**	**0.3**	**0.2**	**0.2**

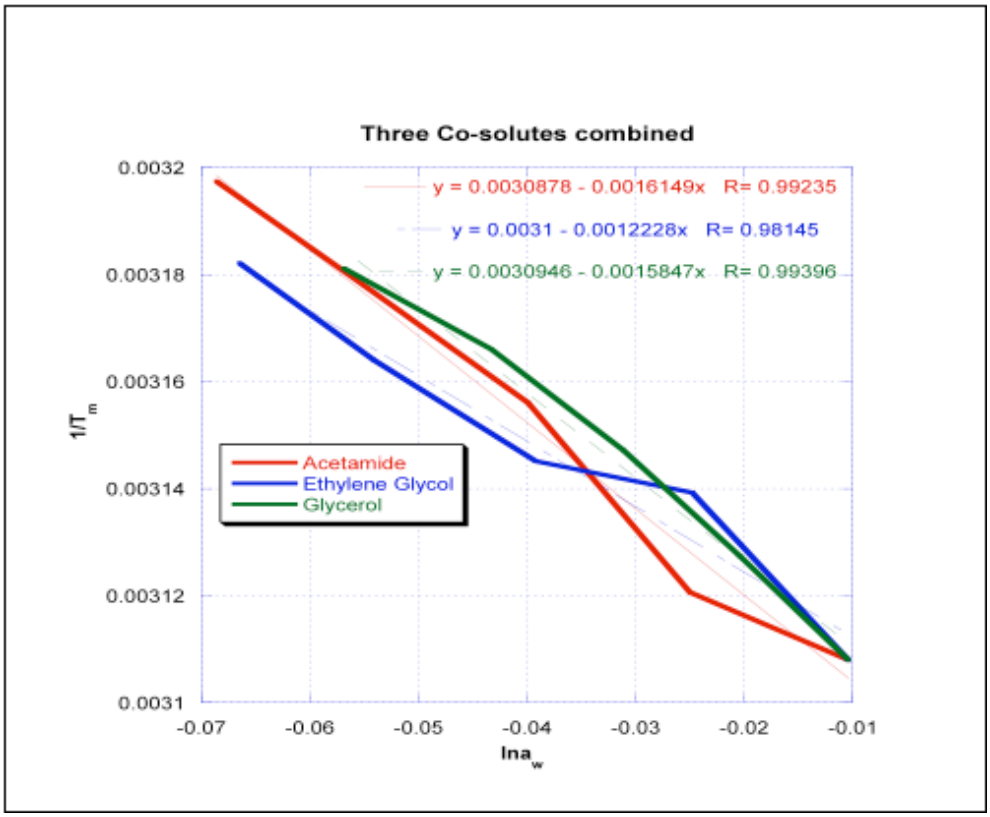

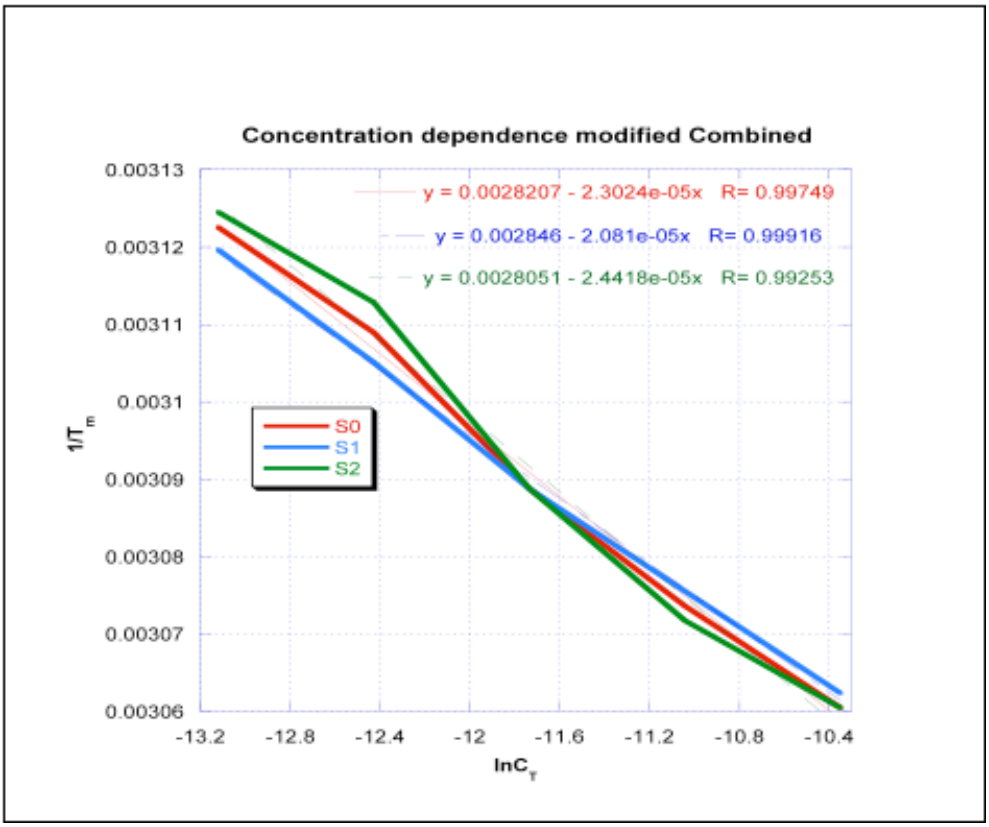

Figure S6. Fitting of the osmotic stress and concentration dependent UV melting data for amide modified **RNA1**.

Table S2. UV thermal melting and osmotic stress data for the unmodified RNA decamer.

File Name	0% Acetamide	5% Acetamide	10% Acetamide	15% Acetamide	20% Acetamide
pt_298A1		57.0	54.1	52.1	49.8
pt_298A2	59.3	57.2	54.1	52.4	50
pt_298B1	58.9	56.9	54.4	52	49.6
pt_298B2	59.5	57.1	54.4	52.2	49.5
pt_299A1	58.7	56.8	54.4	52.3	49.7
pt_299A2	59.2	57	54.3	52.2	49.5
pt_299B1	58.7	57.0	54.1	52.4	49.4
pt_299B2	59.2	56.7		52.4	49.5
Average	**59.1**	**57.0**	**54.3**	**52.3**	**49.6**
STDEV	**0.3**	**0.2**	**0.2**	**0.2**	**0.2**

File Name	0% Ethylene Glycol	5% Ethylene Glycol	10% Ethylene Glycol	15% Ethylene Glycol	20% Ethylene Glycol
pt_054A1		57.9	55.1	53.5	51.9
pt_054A2		57	55.1	53.7	52.2
pt_054B1		57.4	55.1	53.6	52.4
pt_054B2		57.5	55.1	53.6	52.0
pt_055A1		57.8	55.1	53.4	51.9
pt_055A2		57.2	55.1	53.3	51.9
pt_055B1		57.5	54.9	53.5	51.9
pt_055B2		57.2	54.6	53.5	52.1
Average		**57.4**	**55.0**	**53.5**	**52.0**
STDEV		**0.3**	**0.2**	**0.1**	**0.2**

File Name		5% Glycerol	10% Glycerol	15% Glycerol	20% Glycerol
pt_057A1		58	57.2	53.2	52.1
pt_057A2		58.7	57.3	53.8	51.8
pt_057 B1		58.4	57.1	53.2	52.3
pt_057 B2		58.4	57.2	53	51.7
pt_061 A1		58.1	56.8	53.2	52
pt_061 A2		58.2	56.6	53.6	51.6
pt_061 B1		58.1	56.9	53.8	52.2
pt_061 B2			57	53.9	
Average		**58.3**	**57.0**	**53.5**	**52.0**
STDEV		**0.2**	**0.2**	**0.4**	**0.3**

van't Hoff plot **Derivative of α curve**

File Name	ΔH	ΔS	T1	T2	ΔH (cal/mol)	ΔG
pt_298A1	93150	-252.8	53.5	65.8	91193	14.8
pt_298A2	92050	-249	53.3	66.4	85723	14.9
pt_298B1	91300	-246.8	53.3	66.3	86357	14.8

pt_298B2	100400	-275	52.6	65.6	85994	15.2
pt_299A1	97900	-266.9	53.3	66.3	86357	15.2
pt_299A2	102200	-279.7	54	66.4	90756	15.5
pt_299B1	99300	-271	53.3	66.7	83878	15.3
Average	**96614**	**-263.0**	**53.3**	**66.2**	**87179.4**	**15.1**
STDEV	**4387**	**13.3**	**0.4**	**0.4**	**2728.9**	**0.3**

Concentration Dependence

File Name	**2 microM**	**4 microM**	**8 microM**	**16 microM**
pt_053A	57.9	59.3	60	61.6
pt_053A	57.3	58.9	60.4	61.8
pt_053B	57.8	59.5	59.9	61.6
pt_053B	57.3	58.7	59.5	62
pt_053C	58	59.2	59.9	61.8
pt_053C	57.4	58.7		61.3
Average	**57.6**	**59.1**	**59.9**	**61.7**
STDEV	**0.3**	**0.3**	**0.3**	**0.2**

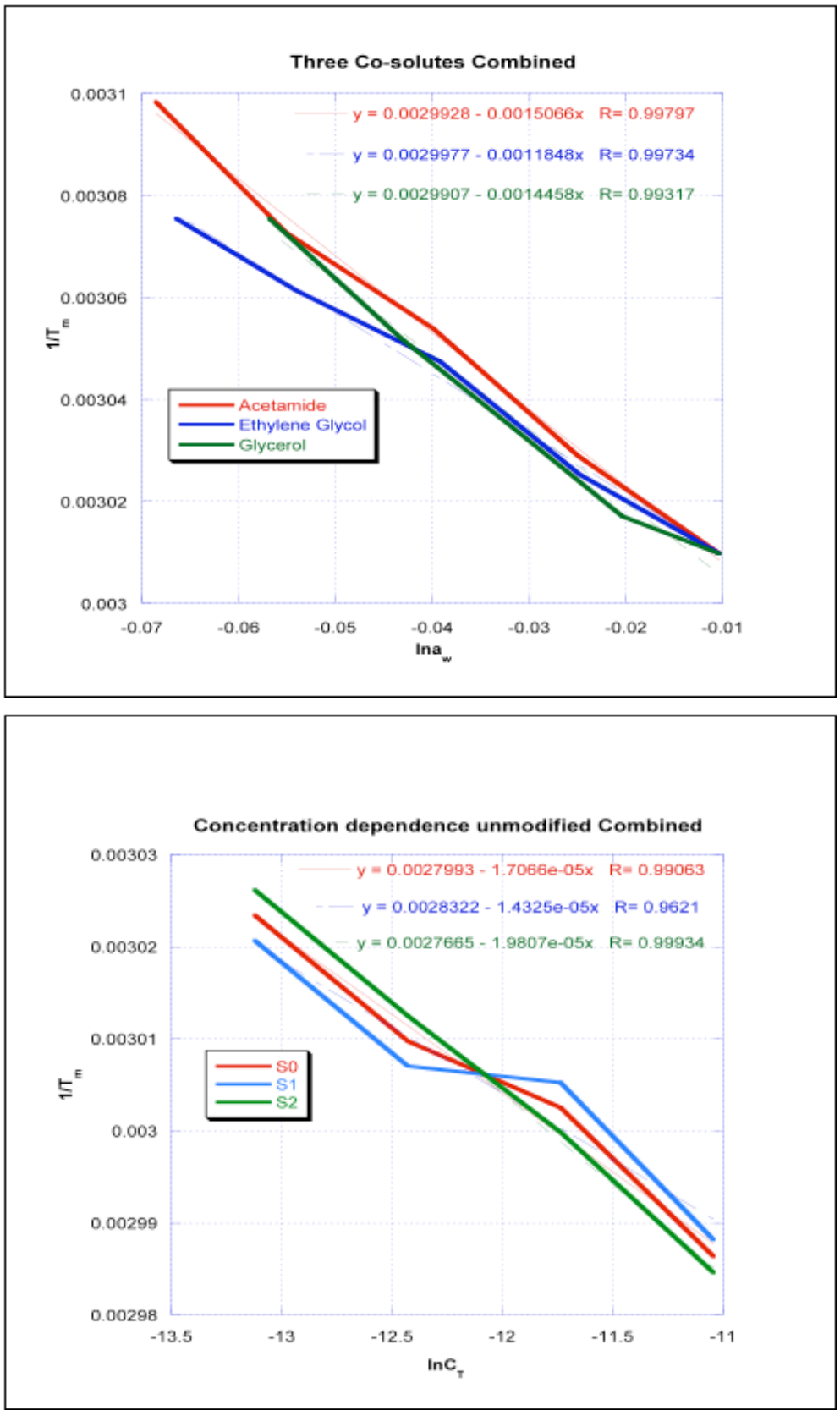

Figure S7. Fitting of the osmotic stress and concentration dependent UV melting data for unmodified RNA decamer.

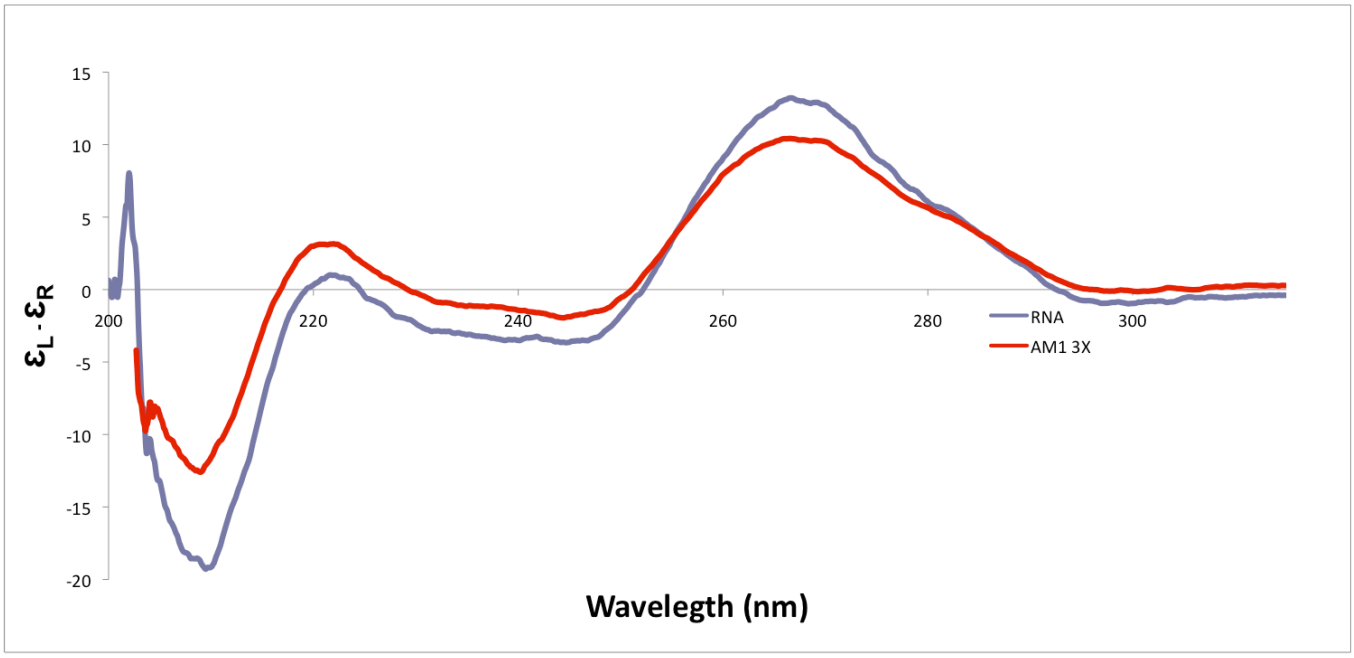

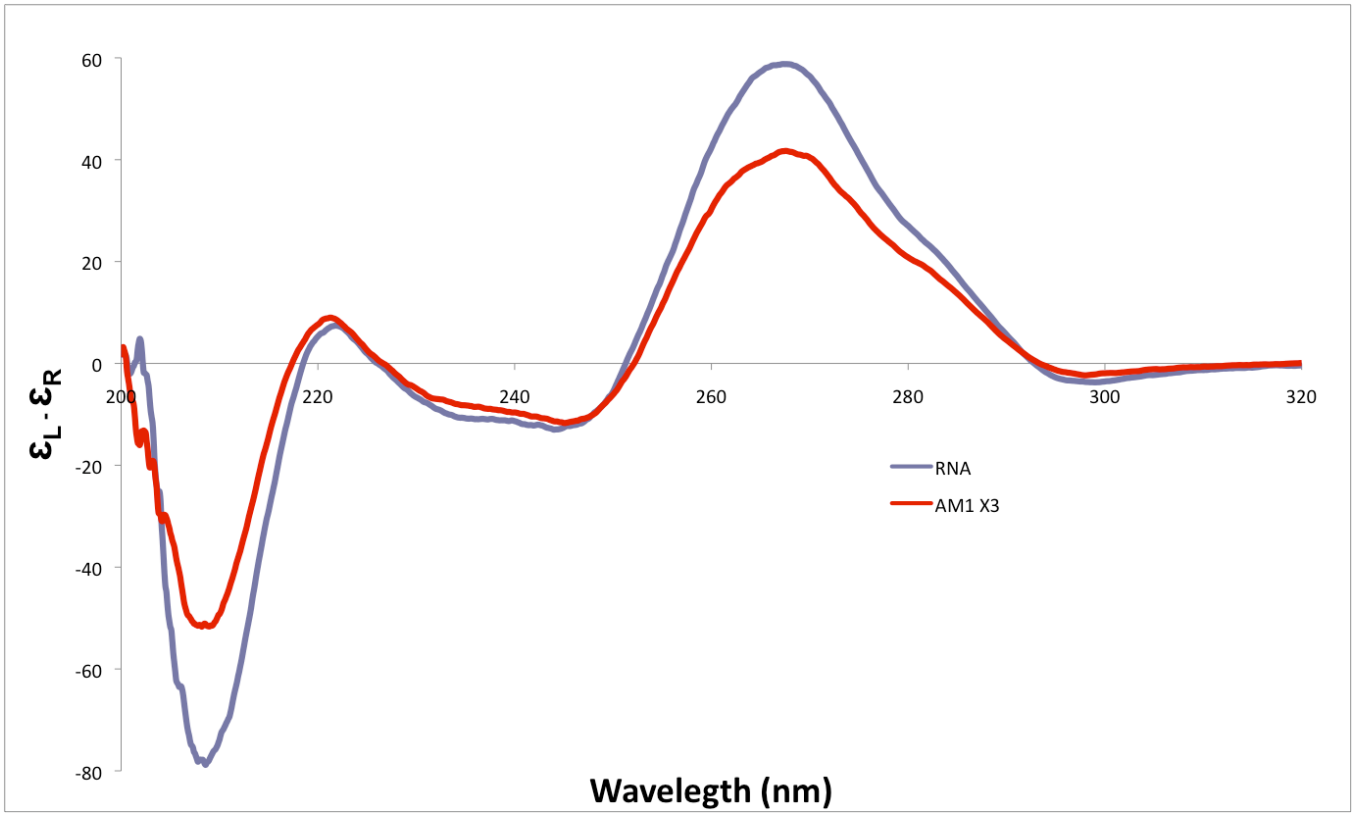

Figure S8. CD spectra of duplex formed by amide-modified **RNA1** and complementary RNA (red) and unmodified control duplex (blue). Upper image: 2 μM of each strand in 10 mM sodium cacodylate, 0.1 mM EDTA, and 300 mM NaCl, pH 7.4 at 10 °C. Lower image: 10 μM of each strand in 10 mM phosphate buffer and 300 mM NaCl, pH 7.4 at 10 °C

NMR Spectroscopy of RNA1. The HPLC purified samples of **RNA1** and the complementary strand were dialyzed against phosphate buffer (20 mM phosphate, 0.08 M NaCl, 50 μM EDTA, pH = 6.3) and dissolved in 0.35 mL of the same buffer. D_2O (5%) was added and the sample was placed in a Shigemi (Alison Park, PA) NMR tube. NMR spectra were acquired on a Varian Inova spectrometer at 600 MHz. 2D NOESY spectra in 95% H_2O/5% D_2O were acquired at 0 and 20 °C with mixing times of 100, 125, and 400 ms. 2D TOCSY spectra were acquired at 0 and 20 °C with mixing time of 28 msec.

NMR spectroscopy revealed a largely A-form conformation of the triple amide-modified duplex. 1D and 2D NMR spectra of the imino protons indicate Watson-Crick pairing through all the expected pairs, including the four AU pairs flanking amide modifications. Formations of GC pairs in the stems is indicated by strong NOEs between G imino and C amino protons, and ~1.5 ppm downfield shift of one of each pair of C amino protons indicating involvement in a hydrogen bond. Formation of the AU pairs is clearly indicated at 0 °C by strong NOEs between the uracil imino and adenine H2 protons and the relatively downfield shifts of the U imino protons (Figure S9, bottom). The loss of the A to U NOEs for the central AU pairs at 20 °C is caused by increased imino-water exchange and suggests greater solvent accessibility and lower stability in this region. Further, medium NOEs between each AH2 proton and two H1' protons (one on each strand) are typical of adenine bases positioned inside a helix (Figure S9, blue labels). All ribose groups exhibit C3'-endo conformation, as indicated by undetectable H1'–H2' scalar coupling (Figure S10). All glycosidic bond angles are in the *anti* conformation as indicated by medium NOEs for intraresidue H8/6-H1' protons. Intraresidue and sequential NOEs typical of an A-form backbone were observed including nH8/6-(n-1)H2', nH8-nH3', and nH8-nH2', although the nUH6-(n-1)H2' distances spanning the three amide-linkages are apparently slightly longer than those spanning phosphate-linkages by about 15% (~0.3 Å) as indicated by NOEs about half the normal amplitude. The continuous NOE "walk" through both strands of the duplex (Figure S9, top) further reflects the A-form backbone.

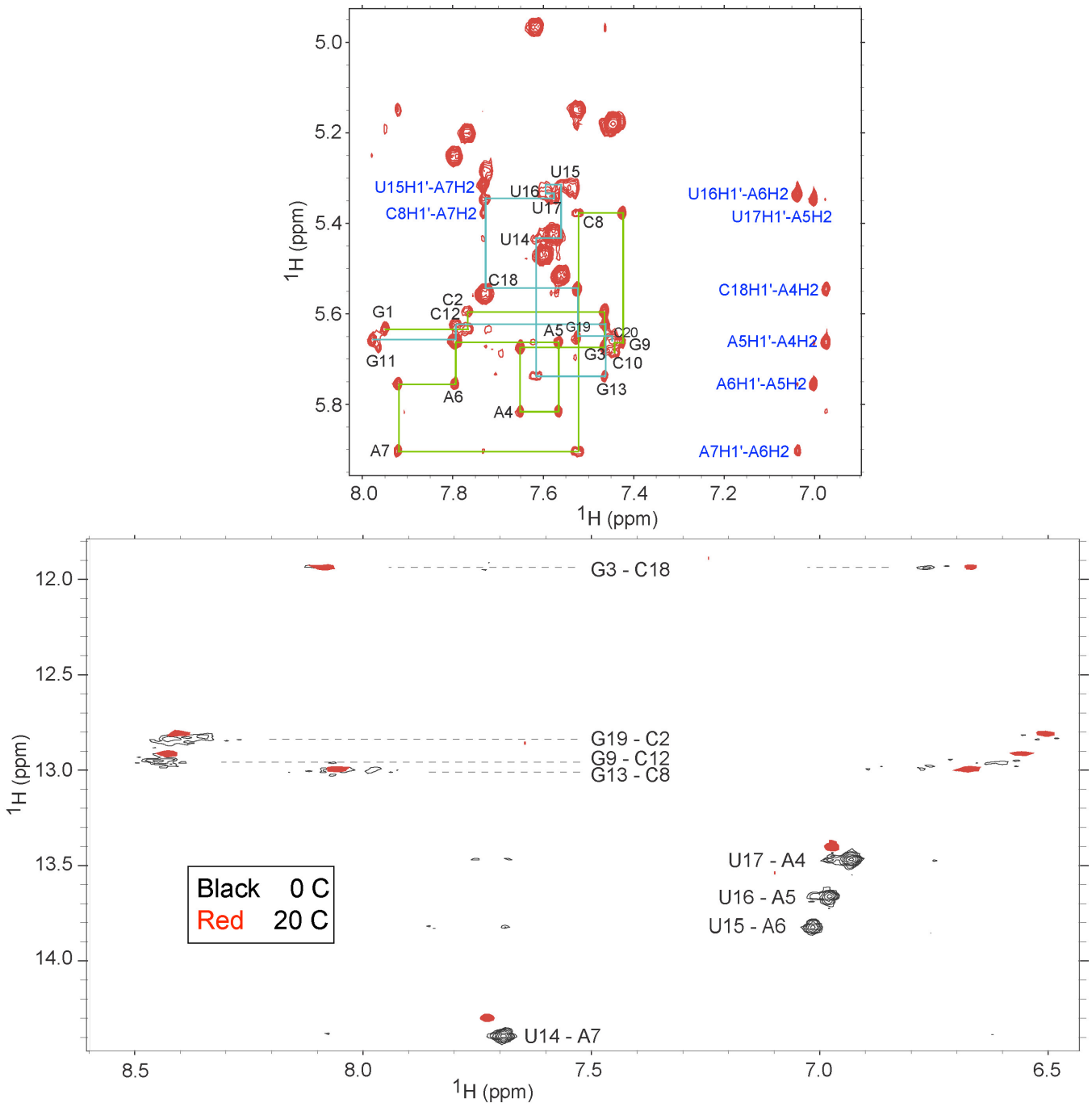

Figure S9. 2D NOESY spectra of duplex of **RNA1** and complementary RNA in buffer (pH 6.3, 80 mM NaCl, 20 mM PO4, 50 μM EDTA, 95%/5% H_2O/D_2O). (top) Aromatic to H1'/H5 cross-peaks at mixing time = 400 msec and 20 °C. Backbone walk of both strands is indicated with connecting lines. Blue labels indicate cross-peaks of each adenine H2 with two H1' protons. (bottom) Imino to aromatic/amino cross-peaks at mixing time =125 msec. Black peaks are at 0 °C and red peaks are at 20 °C. Labels indicate cross-peaks from adenine H2 to paired, modified-U imino, and C amino to paired G imino. At 20 °C H3 protons for U16 and U15 exchange rapidly with water leading to weaker (missing) NOEs with AH2s than observed for U17 and U14.

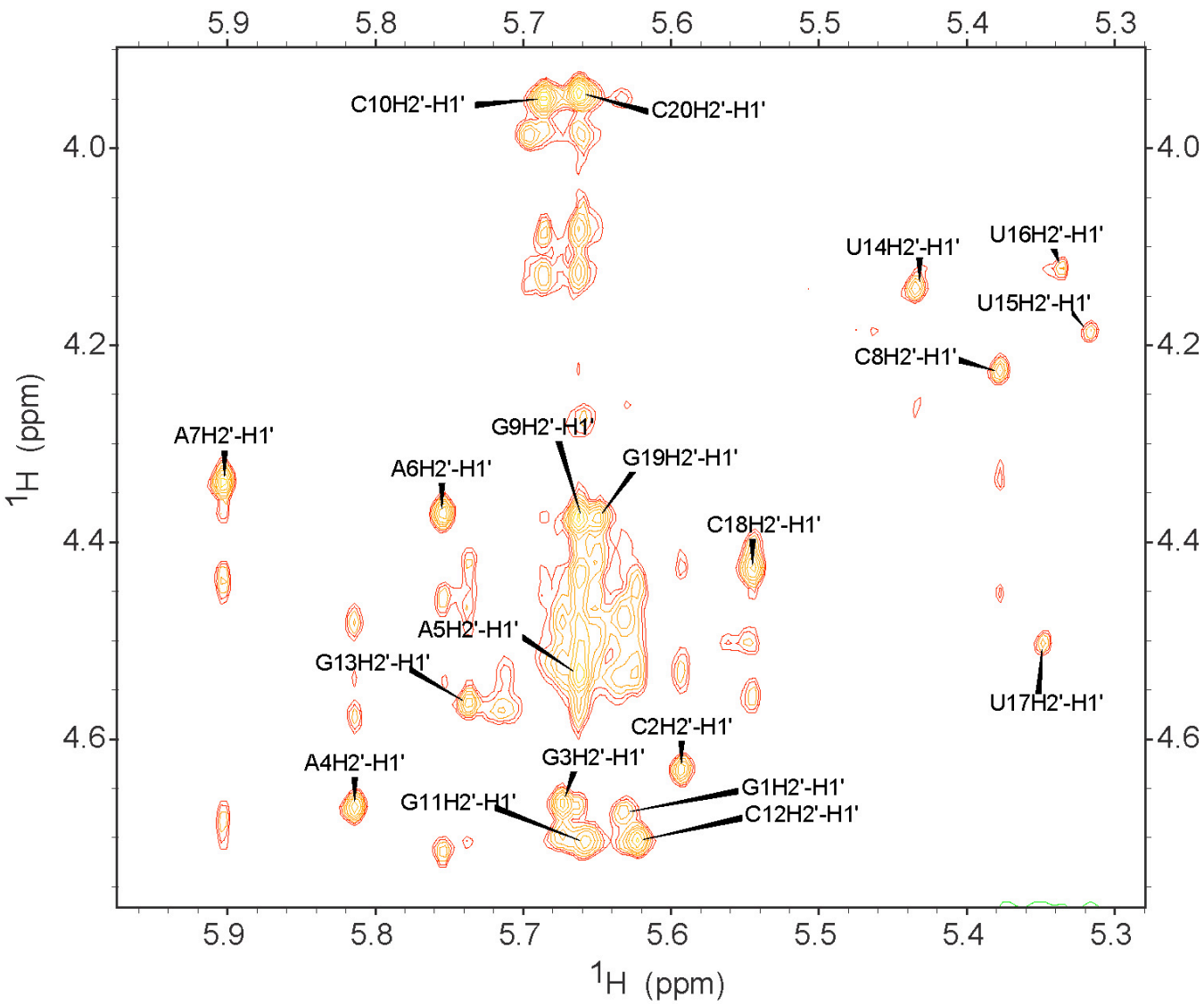

Figure S10. 2D NOE of duplex of **RNA1** and complementary RNA in buffer at 20°C showing H1' - H2' cross-peaks. The narrow H1' resonances indicate lack of scalar coupling to H2' and, therefore, that all sugars are C3´-endo. Mixing time is 400 msec.

Due to the limited quantity of sample, complete NMR assignments were not obtained. Nonetheless, complete proton assignments were obtained for the four U residues adjacent to the amide linkages (with the exception of U14 H5′ and H5′′, which presumably have shifts overlapping all the other H5′/5′′ protons adjacent to phosphate linkages). Assignments of all other residues were missing only H3′, H4′, and H5′/5′′ protons (Table S3). The conformation of the torsion angles within the amide-linkages could not be determined directly from measurement of scalar couplings because overlap of H6′/6′′, H5′/5′′, and H3′ protons of the three U residues precluded accurate measurements. Instead, NOEs between sugar protons and the amide protons, combined with molecular modeling identified the dominant conformations. Amide protons in each modified linkage show very weak or missing NOEs to H2′ and H3′ of the residue 5′ of the amide and a medium NOE to H4′ of the 3′ residue (Figure S11). Simulated annealing carried out with these and other NOE restraints clearly excluded some conformations that were energetically allowed by the molecular dynamics force field. In particular, some *cis* conformations of the amide bond and *trans* conformations in which the plane of the amide bond is flipped by 180° relative to the dominant models are ruled out by the weak nUHN-(n-1)UH2'/H3' cross-peaks. The NOE patterns between the amide protons and sugar protons observed for this triple amide-modified duplex are very similar to those observed in the duplex with a single amide linkage previously studied.[4] The amide conformation determined for the single amide linkage, which was supported by torsion angles determined from scalar coupling data, is the same as the dominant conformation determined for the current triple-amide construct. All distance information obtained from NOE spectra is given in Table S4.

In the single amide-modified duplex in our previous study, $J_{H4'H5'}$ and $J_{H4'-H5''}$ indicated that the gamma dihedral angle adjacent to the amide linkage was in the non-A-form trans conformation, instead of the usual *gauche*+ conformation. The *trans* conformation is also indicated by the relatively strong intraresidue H6-H5′′ NOE (relative to A-form), and that the H4′-H5′ NOE is greater than the H4′-H5′′ NOE. While $J_{H4'H5'}$ and $J_{H4'H5''}$ are not definitively measured in the triple-amide duplex, the same H6-H5′′ NOE pattern is observed as in the single modification. Accordingly, the models resulting from restrained simulated-annealing yield trans conformations of the gamma angle in all three amide-linkages.

[4] Selvam, C.; Thomas, S.; Abbott, J.; Kennedy, S. D.; Rozners, E. *Angew. Chem., Int. Ed.* **2011**, *50*, 2068-2070.

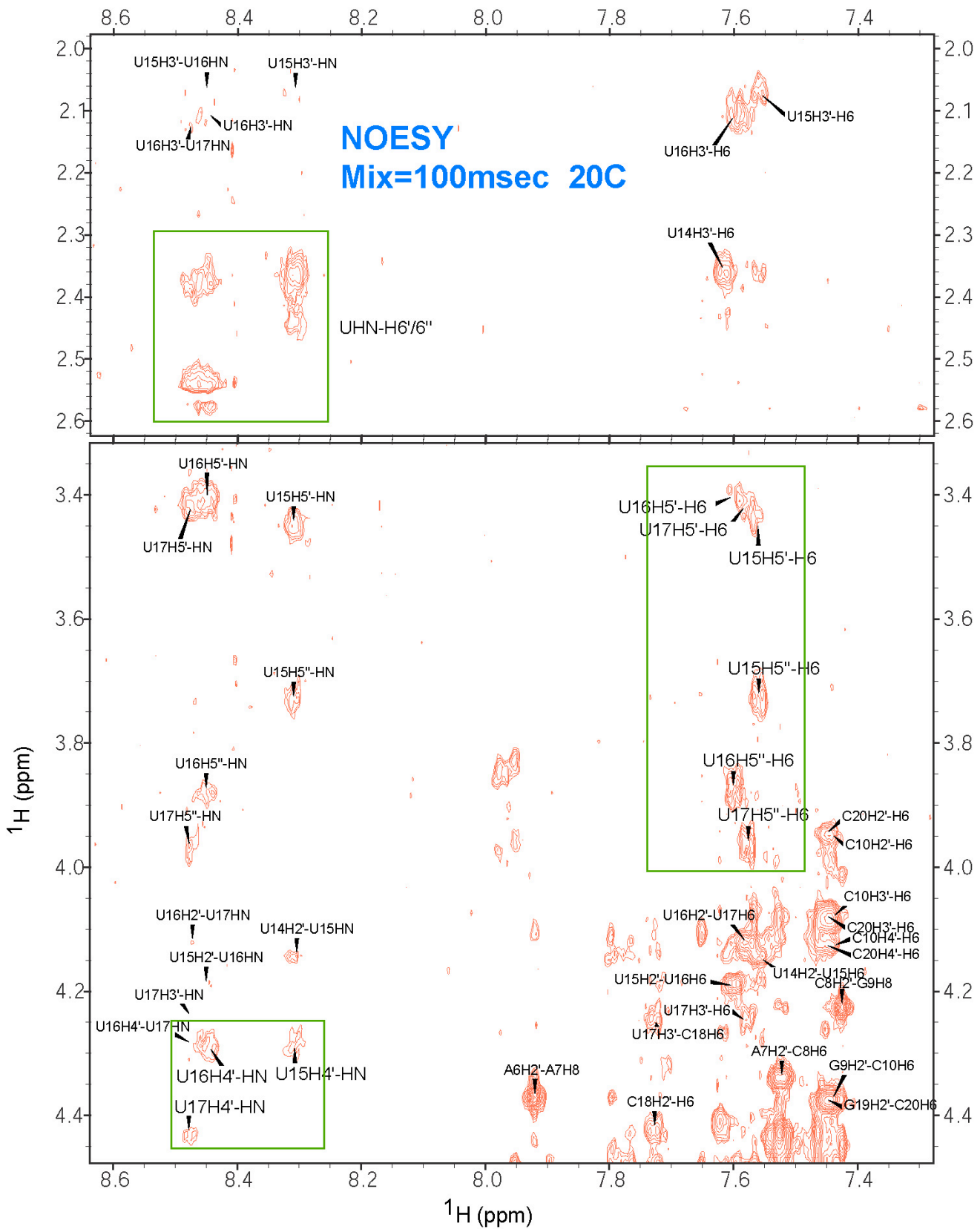

Figure S11. 2D NOE showing HN and H6 to sugar protons.

Table S3. NMR proton chemical shifts at 20 °C and pH 6.3 for duplex of **RNA1** and complementary RNA.

	H1'	H2'	H3'	H4'	H5'	H5''	H5/H2	H6/H8	H1/H3	HN
G1	5.633	4.675	-	-	3.955	3.834	na	7.951	-	na
C2	5.595	4.631	-	-	-	-	5.199	7.768	na	na
G3	5.673	4.665	-	-	-	-	na	7.464	11.94	na
A4	5.814	4.67	-	-	-	-	6.975	7.651	na	na
A5	5.661	4.535	-	-	-	-	7.002	7.567	na	na
A6	5.755	4.372	-	-	-	-	7.036	7.796	na	na
A7	5.902	4.339	-	-	-	-	7.732	7.92	na	na
C8	5.376	4.226	-	-	-	-	5.149	7.524	na	na
G9	5.662	4.377	-	-	-	-	na	7.425	12.92	na
C10	5.686	3.949	4.083	4.125	-	-	5.182	7.445	na	na
G11	5.658	4.704	-	-	3.976	3.848	na	7.977	-	na
C12	5.625	4.703	-	-	-	-	5.253	7.794	na	na
G13	5.738	4.563	-	-	-	-	na	7.464	13.00	na
U14	5.431	4.143	2.36	4.262	-	-	4.967	7.617	14.31	na
U15	5.315	4.189	2.069	4.282	3.442	3.724	5.514	7.559	13.71	8.308
U16	5.333	4.122	2.107	4.285	3.406	3.872	5.47	7.598	13.56	8.45
U17	5.347	4.502	4.243	4.43	3.415	3.966	5.425	7.577	13.41	8.475
C18	5.545	4.427	4.556	-	-	-	5.557	7.728	na	na
G19	5.65	4.376	-	-	-	-	na	7.524	12.82	na
C20	5.662	3.946	4.077	4.125	-	-	5.175	7.45	na	na

na: not applicable

Table S4. NMR derived distance restraints (Å) used to model duplex of **RNA1** and complementary RNA. The majority involve the AU pairs with amide-modification. In addition to these, hydrogen bond restraints were set for all ten base pairs (26 hydrogen bonds).

Atom A		Atom B		Lower	Upper	Atom A		Atom B		Lower	Upper
G1	H1'	G1	H8	2.89	4.61	U15	H3'	U15	HN	3.00	99.00
G1	H2'	C2	H6	2.01	3.20	U15	H3'	U16	HN	2.70	99.00
G3	H2'	A4	H8	1.92	3.06	U15	H4'	U15	HN	2.31	3.69
A4	H1'	A4	H8	3.03	4.84	U15	H5"	U15	H6	2.09	3.34
A4	H2'	A5	H8	1.96	3.12	U16	H1'	A6	H2	2.41	3.84
A5	H1'	A4	H2	2.41	3.84	U16	H2'	U17	H6	2.06	3.29
A5	H1'	A5	H8	2.96	4.72	U16	H2'	U17	HN	3.00	5.00
A6	H1'	A5	H2	2.67	4.26	U16	H3'	U16	HN	3.00	99.00
A6	H2'	A7	H8	1.83	2.92	U16	H3'	U17	HN	2.70	99.00
A7	H1'	A6	H2	2.77	4.41	U16	H4'	U16	HN	2.35	3.74
A7	H1'	A7	H8	2.93	4.68	U16	H5"	U16	H6	2.07	3.30
A7	H2'	C8	H6	1.92	3.06	U17	H1'	A5	H2	2.39	3.81
C8	H1'	A7	H2	2.73	4.36	U17	H2'	C18	H6	1.92	3.06
C8	H2'	G9	H8	1.84	2.94	U17	H3'	U17	H6	2.35	3.74
G9	H2'	C10	H6	1.88	3.00	U17	H3'	U17	HN	3.00	99.00
G11	H1'	G11	H8	2.91	4.64	U17	H4'	U17	HN	2.73	4.36
C12	H2'	G13	H8	1.86	2.97	U17	H5"	U17	H6	2.16	3.45
G13	H1'	G13	H8	3.08	4.91	C18	H1'	A4	H2	2.64	4.21
G13	H2'	U14	H6	1.81	2.89	C18	H2'	C18	H6	2.20	3.50
U14	H2'	U15	H6	2.06	3.29	G19	H1'	G19	H8	3.07	4.89
U14	H2'	U15	HN	3.00	5.00	G19	H2'	C20	H6	1.88	3.00
U15	H1'	A7	H2	2.20	3.51	U15	H3	A7	H2	3.00	5.00
U15	H2'	U16	H6	2.06	3.29	U16	H3	A6	H2	3.00	5.00
U15	H2'	U16	HN	3.00	5.00	U17	H3	A5	H2	3.00	5.00

Molecular Modeling of RNA1 with NMR derived restraints. A representative model resulting from simulated-annealing with the relatively small number of restraints obtained from the duplex of RNA1 and complementary RNA is shown in Figure S12. The backbone is shown overlayed on an xray structure of dsRNA composed entirely of AU pairs (PDB ID 1H1K).

Restraint Generation

Distance restraints were generated from cross-peaks in 100 ms mixing time NOESY spectra at 0 and 20°C using $(1/r)^6$ scaling. Cross-peaks from H5-H6 (2.45 Å) in the Watson-Crick stems were used for reference volumes. Upper and lower limits of the distance restraints allowed for a three-fold error of the NOE volume. Watson-Crick hydrogen-bond restraints (donor-acceptor distance of 1.8 – 2.4 Å) were

applied between all ten base pairs as indicated by imino proton cross-peaks in NOESY spectra. The absence of H1′-H2′ peaks in TOCSY spectra indicated C3′-endo sugar puckers. Backbone dihedrals in the GC stems were assumed to be A-form and were restrained to: α (-65 ± 90°), β (165 ± 75°), γ (60 ± 60°), ε (-115 ± 125°), ζ (-70 ± 90°) as defined previously (Richardson, J. S., Schneider, B., Murray, L., Kapral, G., Immormino, R., Headd, J., Richardson, D., Ham, D., Hershkovits, E., Williams, L., Keating, K., Pyle, A., Micallef, D., Westbrook, J., and Berman, H. *RNA* **2008**, 14, 465-481). Backbone dihedral angles within the AU pairs were not restrained (with the exception of δ). All glycosidic bonds were loosely restrained to *anti* (255 ± 85°) because no large H8/H6-H1′ NOE cross-peaks were observed.

Structure Calculation

Simulated annealing and molecular dynamics calculations were carried out using distance and dihedral angle restraints described above. The structures were calculated using the program AMBER (version 10, AMBER99 force field) with Generalized-Born implicit solvent. New uracil residues with the amide linkage modification were generated using already existing atom types and corresponding bond, angle, and dihedral force parameters (gaff.dat). Atom partial charges were estimated from those for a glycine residue. The simulated annealing protocol was as follows: the system was heated to 3000 K followed by slow cooling to 0 K over 100 ps in steps of 1 femtosecond using NOE and dihedral scale factors of 30 kcal/mol Å2 and 30 kcal/mol rad2, respectively. A total of 50 structures were calculated in this way from randomized initial atom velocities. The resulting 50 structures were subjected to a second round of simulated annealing with heating only to 600 K, Twelve structures without distance and dihedral violations (> 0.2 Å/2°) and with total restraint energies less than 1 kcal were selected from this set. Coordinates are deposited with the Protein Data Bank.

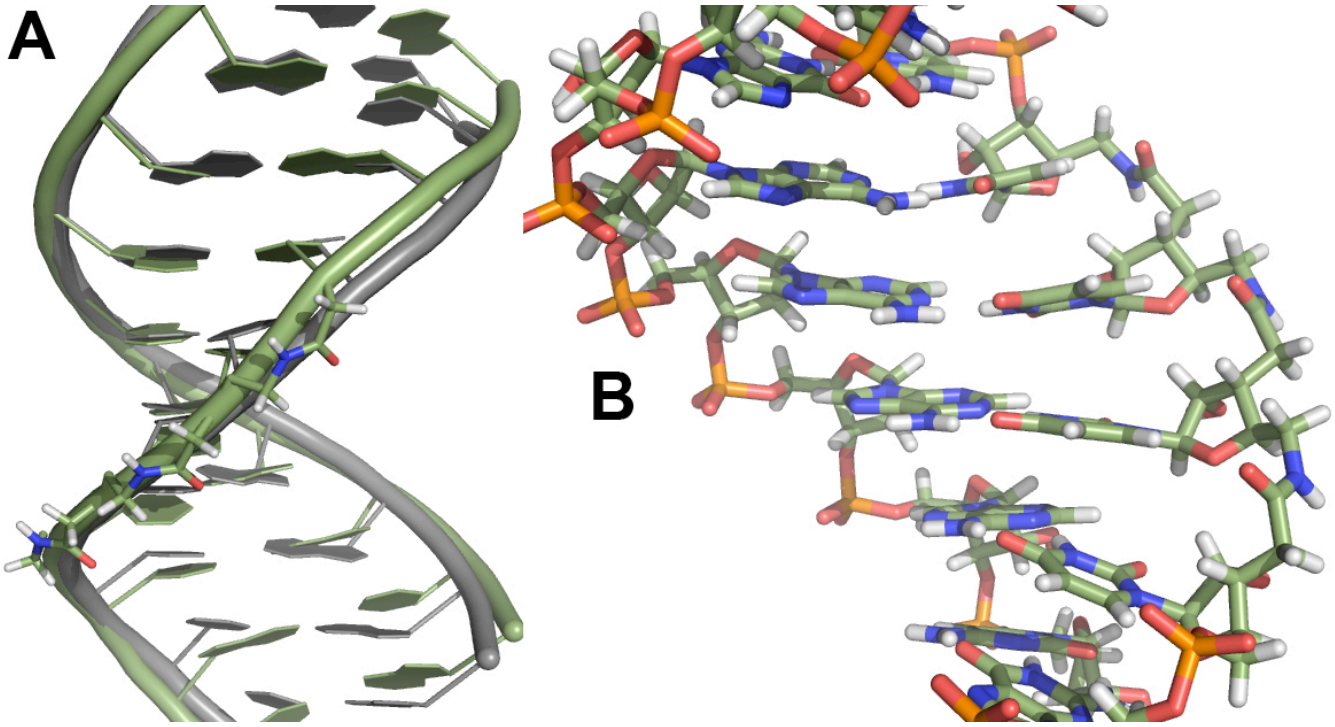

Figure S12. A model of duplex formed by **RNA1** and a complementary RNA strand: **A** model (green) overlaid with PDB 1H1K (grey), the dominant orientation of the amide linkages is indicated; and **B** major groove view of the modified UA tract (amide backbone on right side).

siRNA activity test: HeLa cells were plated in 96-well plates (1 x 10^4 cells/well) for 24 h before transfection. On the day of transfection, RNA-lipid complexes were introduced into each well of cells (0.1-100 nM RNA for HeLa cells 0.2 mL/well DharmaFECT 1) Twenty-four h post-transfection, the level of target knockdown was assessed using a branched DNA assay according to manufacturer's instructions (QuantiGene branched DNA signal amplification kit; Panomics, Fremont, CA) specific for the targets of interest. Cell viability was determined using an alamarBlue assay (BioSource Intl, Inc.) according to manufacturer's instructions (Figure S14).

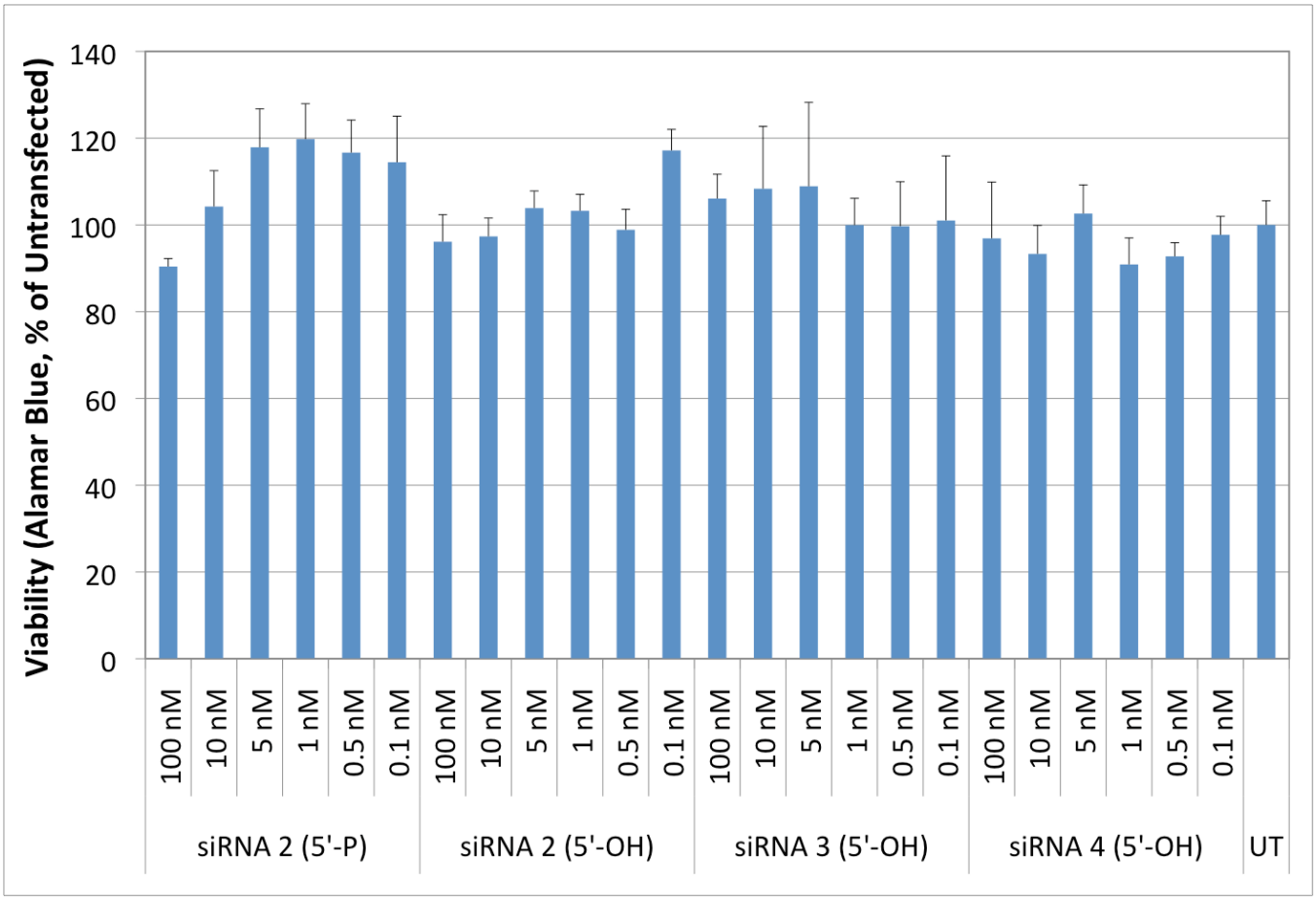

Figure S13. Cell viability determined using an alamarBlue assay.

Label	Assigned Value
1	1.00
2	0.98
3	1.01
4	1.03
5	1.06
6	0.96
7	2.00
8	0.98
9	1.03
10	23.18

H-1 in chloroform-d
Azido Tom Uridine
ppm

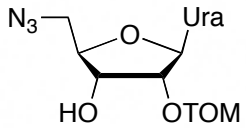

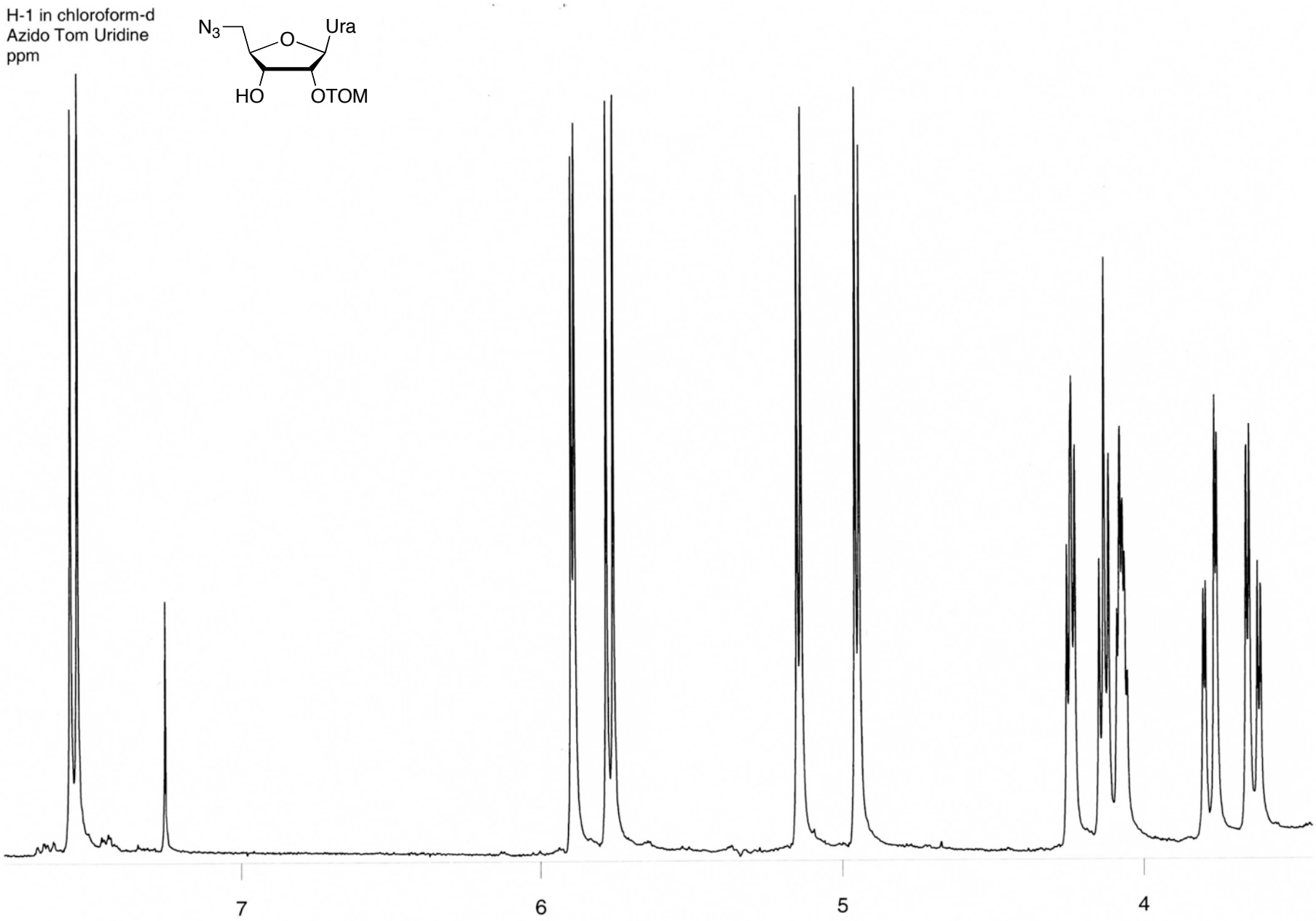

C-13 NMR Spectrum in Chloroform-d
Azido TOM Uridine
ppm

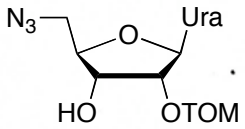

Label	Assigned Value
1	1.00
2	2.00
3	2.04
4	1.00
5	0.91
6	4.97
7	2.06
8	21.21

H-1 in chloroform-d
Amino TOM Uridine
ppm

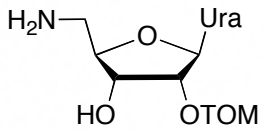

5

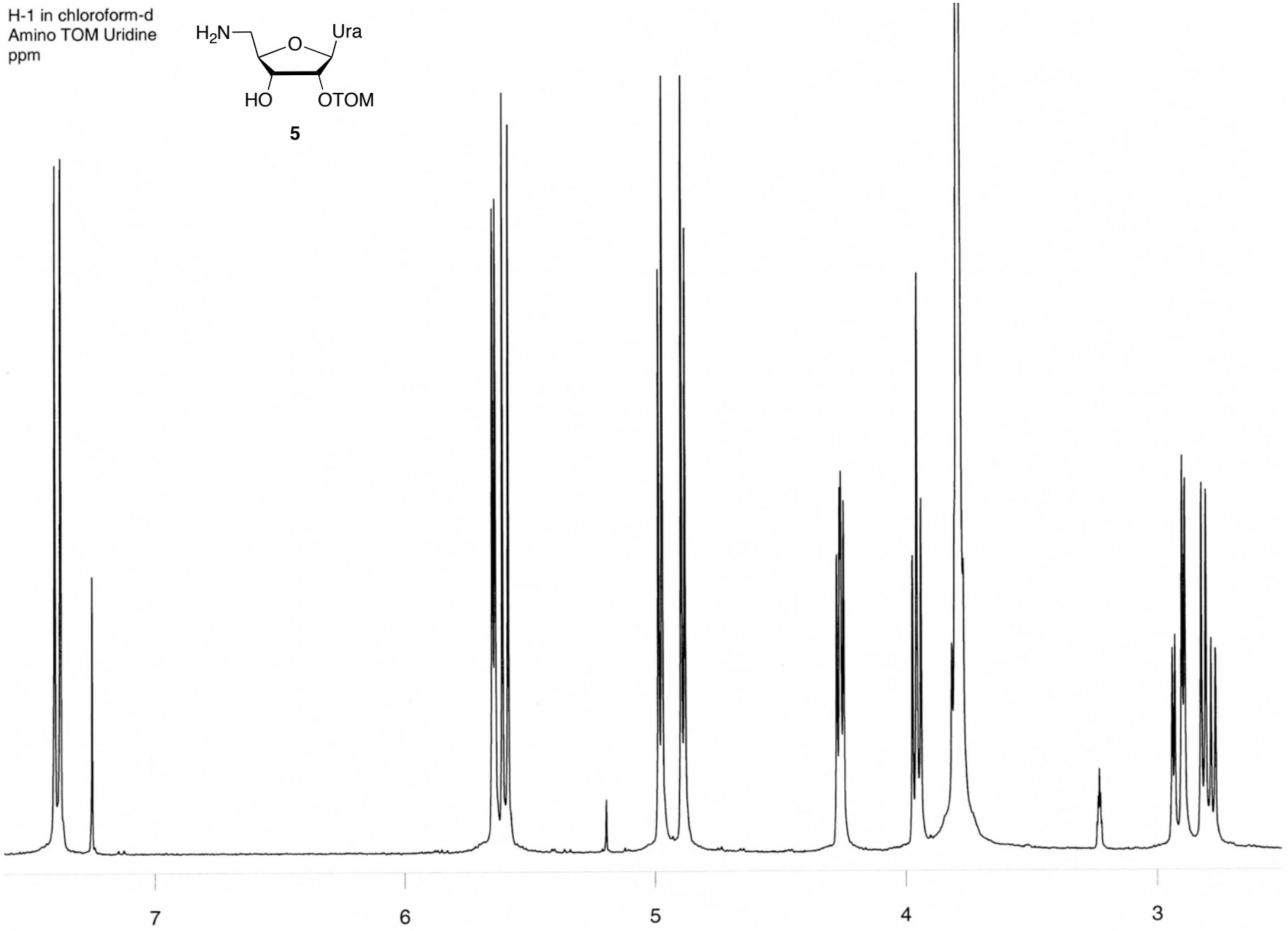
H-1 in chloroform-d
Amino TOM Uridine
ppm
H2N
O
Ura
HO
OTOM
5
7
6
5
4
3

C-13 NMR Spectrum in Chloroform-d
Azmino TOM Uridine
ppm

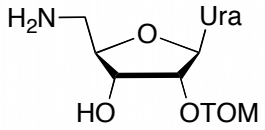

5

Label	Assigned Value
10	14.44
11	2.23
12	1.10
13	1.10
14	1.08
15	1.13
16	2.20
17	1.06
18	3.00
19	1.26
20	1.23
21	23.07

H-1 in chloroform-d
MMTr U TOM
ppm